

Flight Planning for Stereo Radar Mapping

This analysis indicates that, with proper selection of flight paths, available radar systems are adequate for medium-scale stereo mapping.

INTRODUCTION

SINCE THE EARLIEST image-like radar displays of terrain details, various cartographers and photogrammetrists have explored the possibility of using airborne imaging radar data for topographic map compilation in order to obtain the advantages of all-weather operation. A special mapping system was developed and deployed by the military for this purpose; however, because this system was rather complex and expensive, efforts to use conventional radar images in the

tion through mensuration of radar images requires that two or more overlapping images be acquired from different flightpaths. A measurement of the across-track position of an imaged feature on a single image corresponds to measurement of the distance from the aircraft (flightpath) to the feature. Two such measurements may be combined through trilateration to compute the position of the feature with respect to points along the flightpaths. This is illustrated in Figure 1 for the commonly used mode employing parallel

ABSTRACT: Pairs of terrain-imaging radar images may be viewed and measured stereoscopically in order to obtain elevation data for topographic mapping. An analysis of the technical and economic considerations in selecting flight parameters for mapping projects is presented. Both parallel and right-angle flightpaths are considered. The results indicate that systems as presently constituted have the potential to produce data adequate for original medium-scale mapping, and that the right-angle mode is superior to the parallel-flightpath mode under the assumptions made if psychophysical difficulties in image fusion are not encountered.

stereo mode have continued. A system having suitable image detail for medium-scale mapping is now commercially available. The Goodyear Aerospace owned-and-operated GEMS^a radar is employed in a twin jet Caravelle aircraft owned and operated by the Aero Service Corporation, a division of Litton Industries. The purpose of this paper is to explore analytically the use of systems of this type in topographic mapping, with particular attention to the relationships between elevation accuracy, cost, and flight parameters.

STEREO MODES

To make a measurement of terrain eleva-

tion through mensuration of radar images requires that two or more overlapping images be acquired from different flightpaths. A measurement of the across-track position of an imaged feature on a single image corresponds to measurement of the distance from the aircraft (flightpath) to the feature. Two such measurements may be combined through trilateration to compute the position of the feature with respect to points along the flightpaths. This is illustrated in Figure 1 for the commonly used mode employing parallel

CONVERGENCE ANGLES

The convergence angles illustrated are a prime variation in flightpath selection. Among the important accuracy limitations to be discussed later are the accuracies of measuring the distances from the flightpaths to the terrain points. As shown in Figure 2, these accuracies combine geometrically to produce an important contribution to eleva-

^a Goodyear Electronic Mapping System.

tion accuracy. Small (weak) convergence angles cause large elevation uncertainty due to range measurement accuracy. The smallest elevation uncertainty, and thus the optimum (strongest) convergence angle from this standpoint, is 90 degrees.

rections. However, radar images viewed from opposite directions have dissimilarities due to illuminating the terrain from the radar. Highlights and shadows are reversed. This causes psychophysical difficulties in fusing the two images into a three-dimensional model. Significant improvements in accuracy are expected from the local averaging which occurs in visual model formation, and more efficient data extraction is possible by using the anaglyphic technique rather than the analytic technique. Furthermore, a prime use of the radar imagery is to view the terrain model stereoscopically in order to perform geologic terrain analysis. Therefore, it is common to use same-side stereo rather than

COMMONLY USED MODE

The mode commonly used employs parallel flightpaths at the same altitude. As shown in the figure, the flightpaths and look direction are ordinarily chosen so that the common area is viewed from the same direction. This has the disadvantage of resulting in weaker convergence angles than would result from choosing to view the area from opposite di-

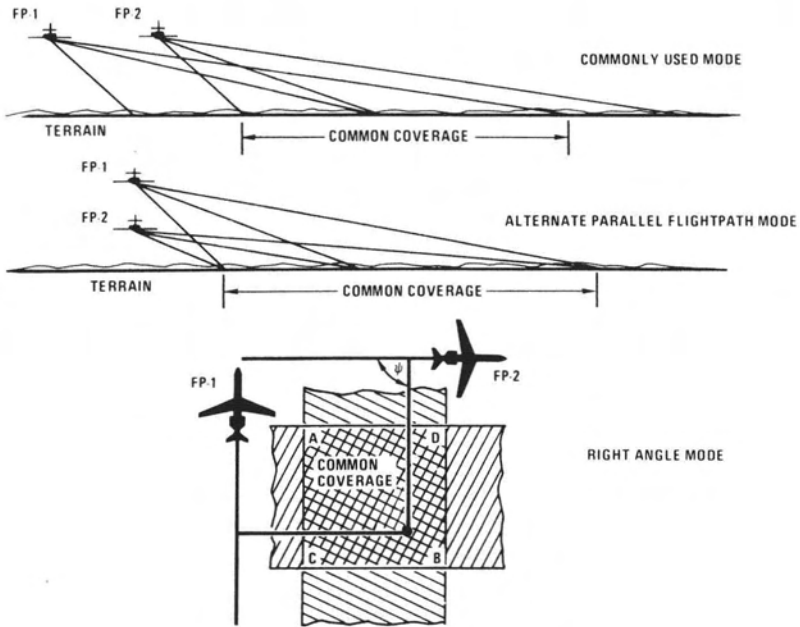


FIG. 1. Stereo modes.

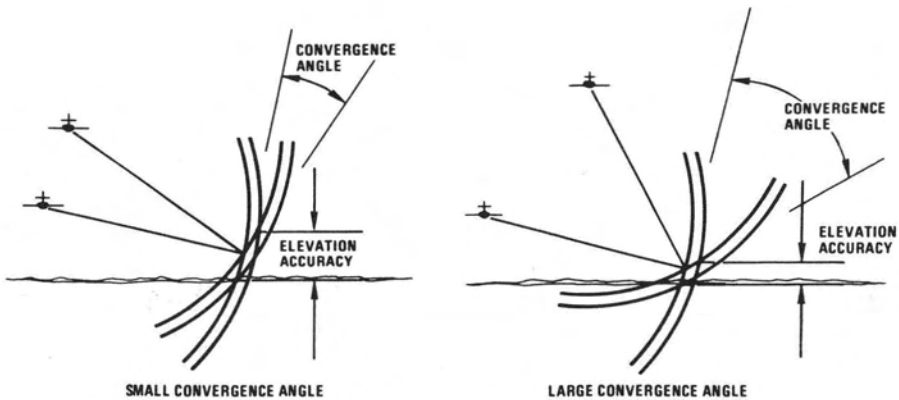


FIG. 2. Convergence angles.

opposite-side stereo in collecting radar imagery.

ALTERNATE PARALLEL FLIGHTPATH MODE

Figure 1 shows the alternate mode in which the parallel paths are flown at different altitudes and are not offset. This mode would, in some cases, produce stronger convergence angles than the commonly used one. However, it suffers from two disadvantages which preclude its use for most work. First, the lower depression angles cause greater terrain masking from elevated terrain, in other words, longer shadows. Second, flying at significantly lower altitudes causes the aircraft to encounter much more turbulence in cloud-covered areas where the radar has greatest utility, which may cause image degradation and danger to flight personnel in severe cases. The alternate mode is not treated further here but those planning stereo flights should be aware of the possibility of using it, or combinations of the two, in special cases. For example, in a low-relief area where the greatest vertical exaggeration possible is desired, two flightpaths offset in both altitude and horizontal position may be used.

RIGHT-ANGLE MODE

It has been known for some time that parallax resulting from any two different flightpaths can be used to create a visual terrain model and to make measurements. Mr. Homer Jensen of Aero Service Corporation has recently suggested that a special case of nonparallel flightpaths be used in terrain analysis and mapping, viz., the case where overlapping coverage is obtained from flightpaths at right angles. This mode has a significant advantage in that the convergence angles are stronger.

On the other hand, the right-angle mode suffers from several disadvantages. First, shadows also fall at right angles and highlights are different, causing difficulties in fusion, although probably not so great as in the opposite side case. Second, parallax, and thus vertical exaggeration and measurement accuracy, vary over the overlap area in both horizontal dimensions rather than in only one (range) as in the parallel cases.

Third, and most important, any lack of orthogonality in the image causes an elevation error. This can be seen in Figure 1 by noting that a deviation from orthogonality in the angle marked ψ by an amount $\delta\psi$ causes an error in the position of the point at B in the image of flightpath 2 by an amount $R\delta\psi$. Approximately the same error would be caused by an error of δR in the measured distance

from flightpath 1. Similarly, an error of $\delta\theta$ in flightpath 1 will cause an error equivalent to δR in distance from flightpath 2. Imaging radars are inherently more accurate in distance measurement than in angular measurement. Thus, there is a tradeoff between the improved strength of the convergence angle and the loss of accuracy due to orthogonality. This is treated in more detail in the following sections, where the potential accuracy of the 90-degree mode is shown to be slightly superior to that of the commonly used mode.

ERROR ESTIMATES

The following sections develop and apply conventional differential calculus estimates for the vertical measurement accuracy in the commonly used parallel flightpath and right-angle modes of radar stereo elevation measurements. Horizontal measurement accuracies could be obtained easily in the same manner. However, vertical measurements are both more stringent in mapping specifications and more difficult to obtain with radar, so that performance level is dependent on these values. Therefore, only the vertical components of terrain measurements are treated, and it can be assumed that horizontal measurements are in general more accurate than the values arrived at here.

ERROR CONTRIBUTIONS

The contributions to vertical measurement accuracy treated here are the principal limitations to the technique and include location of the aircraft in the along-track, across-track, and vertical directions, the accuracy of measuring distance from the flightpath to the terrain (range measurement accuracy), and in the right-angle case, the orthogonality of each image.

HORIZONTAL FLIGHTPATH MEASUREMENT ACCURACY

The GEMS system employs a SHORAN navigation system for measurement of aircraft position. In this system, an airborne transmitter transmits pulses of radio frequency (UHF) energy simultaneously to two ground transponders. The transponders amplify and retransmit the signals back to the aircraft. An airborne receiver and time comparator measure the elapsed time, and thus distance, to each ground station. The transponders are placed far enough from the aircraft so that the difference between ground distances and the slant distance measured are small, and can be corrected, if necessary, by knowing aircraft altitude as described in the next section.

From these two measurements, aircraft position is calculated by trilateration every mile or so along the flight track. An inertial navigator is used to interpolate between the SHORAN "fix" points.

SHORAN system accuracy is a function of equipment calibration, operator proficiency, and the degree to which the radio transmission paths (propagation velocity) are measured and used to correct the raw data. Accuracies of 30 meters^a or so are routinely obtained and 10-meter accuracy is achievable.

Ground station locations are obtained from local ground control or from Transit satellite Geoceivers and are, in general, good enough to be neglected. The error of the inertial system interpolation can also be made small enough to be neglected.

VERTICAL FLIGHTPATH MEASUREMENT ACCURACY

Aircraft altitude above the datum plane is measured by a differential barometric altimeter calibrated during the flight with a radar altimeter. In addition to basic instrument accuracy, the accuracy of this technique depends on proximity of available altitude check points (seashore, lakes, or plains of known elevation) and on the temporal and spatial variation of the isobaric surfaces. Again, accuracies of 30 meters are routinely obtained and 10-meter accuracy is achievable in special conditions.

RADAR RANGE MEASUREMENT ACCURACY

Flightpath-to-terrain distances are measured by scaling the radar imagery. Range marks which represent previously determined distances are generated by a crystal oscillator and displayed in the imagery. Terrain features are measured with respect to this scale, which may be made sufficiently closely spaced so that interpolation errors between marks may be neglected. This is a basic time measurement and with sufficient calibration may be made without difficulty to an accuracy equivalent to the radar's resolution, or about 15 meters in the GEMS case, and to perhaps one-fifth of this value, or 3 meters, with special care and calibration.

ORTHOGONALITY

In the right-angle mode, the largest contributor to elevation error is the lack of complete orthogonality in the imagery, as discussed earlier. The orthogonality is obtained by

^a Accuracies used here are assumed to be one sigma (1σ). The sources do not always state the level specified and this assumption will in some cases be conservative.

doppler signal sensing and an accuracy of about one-tenth of the antenna physical beam, or 0.1 degree is usually achieved.

PARALLEL FLIGHTPATH ELEVATION ERROR

The geometry of an individual stereo measurement is illustrated in Figure 3. From the figure, the x and z position of the imaged point may be determined by simultaneous solution of equations representing circles of radius R₁ and R₂ centered at the flightpaths of positions a₁b₁ and a₂b₂. Thus,

$$R_1^2 = (x - a_1)^2 + (z - b_1)^2$$

$$R_2^2 = (x - a_2)^2 + (z - b_2)^2. \quad (1)$$

The effects of vertical measurement errors in R₁, R₂, a₁, b₁, a₂, and b₂ may be determined by implicit partial differentiation of Equations 1 with respect to these quantities, and simultaneous solution for dz. Treating range measurement accuracy first:

$$2R_1 dR_1 = 2(x - a_1) dx + 2(z - b_1) dz,$$

$$2R_2 dR_2 = 2(x - a_2) dx + 2(z - b_2) dz. \quad (2)$$

Eliminating dx and letting

$$x - a_1 = G_1,$$

$$x - a_2 = G_2,$$

$$G_2 - G_1 = S,$$

$$z - b_1 \approx z - b_2 = h,$$

then

$$dz = \frac{R_1 G_2}{hS} dR_1 - \frac{R_2 G_1}{hS} dR_2.$$

Now if the differentials represent errors in R, which are approximately equal in magnitude but statistically independent,

$$\sigma_z^2 = \frac{(G_1^2 R_2^2 + G_2^2 R_1^2)}{h^2 S^2} \sigma_R^2. \quad (3)$$

Similarly,

$$\sigma_x^2 = \frac{2G_1^2 G_2^2}{h^2 S^2} \sigma_a^2,$$

$$\sigma_x^2 = \frac{G_1^2 + G_2^2}{S^2} \sigma_b^2.$$

The flight parameters for the GEMS system in its normal mode are h=12 km, s=15 km so that the overlap is represented by

$$9 \text{ km} < G_2 < 31 \text{ km},$$

$$24 \text{ km} < G_1 < 46 \text{ km}.$$

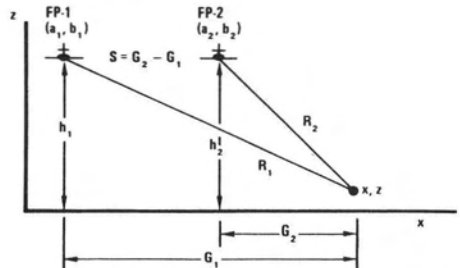


FIG. 3. Parallel flightpath measurement geometry.

Using the accuracy estimates stated earlier, we may characterize the values conveniently achieved as realistic and those achievable with greater care and calibration as optimistic, as follows:

Error contribution	Realistic value	Optimistic value
σ_R	15 m	3 m
σ_a, σ_b	30 m	10 m

Using these values in Equation 3 and taking the RMS σ_z (the three contributions to the variance are summed), the curves in Figure 4 are obtained, where σ_z is plotted as a function of ground distance to the nearest flightpath, G_2 . It may be noted that the realistic values produce an average error of about 200 m and the optimistic around 70 m. Choosing 100 m as the approximate requirement for medium scale mapping, the predicted results are probably too close to the optimistic end to regard this as a capability based on single stereo measurements. However, no advantage has been taken of accuracy improvements from ground control incorporated as block adjustments. This improvement, realizing that some of the values used in arriving at Figure 4 are conservative, indicates that available equipment is suitable for medium-scale mapping. Possible accuracy improvement through additional or alternate data collection and reduction are described in the following section.

REDUNDANT FLIGHTPATHS

The spacing between flightpaths used in generating Figure 4 was chosen to provide about 60 per cent sidelap. That is, just enough

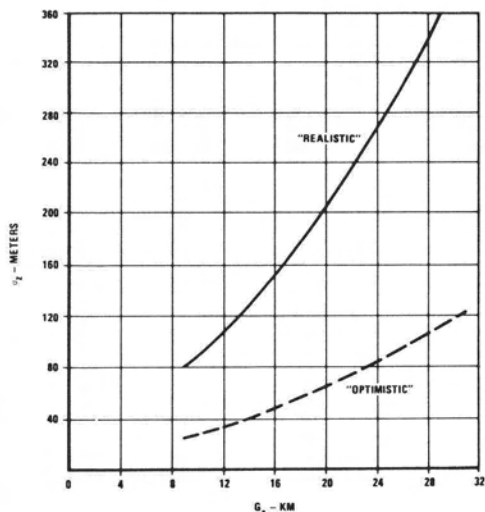


FIG. 4. Elevation error, normal stereo, $S=15$ km.

to ensure duplicate coverage of terrain with allowance for navigation errors and elevation displacement with the 37 km swath available. If the spacing is reduced somewhat, then measurements may be made between alternate flightpaths and the spacing increased to about two-thirds of the swath rather than half, thus providing a stronger convergence angle. Furthermore, the use of both adjacent and alternate flightpaths provides redundancy to improve the accuracy even further. If the terrain is imaged n times, the maximum flightpath space is $n-1/n$ (swath), approaching the total swath for large n and providing $n-1$ redundant (but not equally accurate) measurements. More combinations of flightpaths are possible, but such measurements are not independent and no further improvement in accuracy (except for that of the final measurement) will result. Therefore, the image from the path nearest the swath, of width $1/n$, should be compared with each remaining image and the results combined. In combining measurements, the results should be weighted according to the inherent accuracy of each for a maximum likelihood estimate. If the accuracy of the various measurements are $\sigma_1, \sigma_2, \dots, \sigma_m$, the resulting accuracy will be:

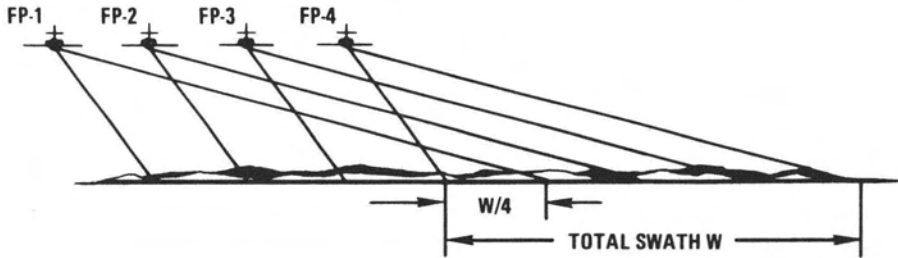
$$\frac{1}{\sigma^2} = \frac{1}{\sigma_1^2} + \frac{1}{\sigma_2^2} + \dots + \frac{1}{\sigma_m^2}.$$

This scheme is illustrated in Figure 5 for $n=4$.

In order to characterize the advantages which may be gained from this procedure, Equations 3 were used to estimate the accuracy attainable with $n=2$ (minimum stereo coverage), $n=3$ and $n=4$. If it is assumed that data collection and data reduction costs are about equal in the normal data collection and reduction mode and calling this value 1, then Table 1 defines the relationship of cost to n , using either complete data reduction, or only the most accurate pair. The average accuracy for $n=2, 3$, and 4 from Equations 3 is given in Table 2.

As noted in the table, both the optimistic and realistic estimates of error contribution have been used, and the computations have been made for altitudes of both 13 km and 6 km. The higher altitude applies to most situations and the lower to mapping of high mountains where the terrain rises to values which significantly reduce effective convergence angles.

To provide a graphic interpretation, these data have been plotted on Figure 6, along with an overall average curve based on arbitrarily selecting the performance parameters halfway between those previously charac-



FLIGHTPATH COMBINATION	S (SPACING)
4-1	3W/4
4-2	W/2
4-3	W/4

FIG. 5. Multiple flightpaths, n=4.

TABLE 1. RELATIONSHIP OF COST TO n.

S*	n	Data collection cost	Data reduction		Total cost	
			All data	Most accurate data only	All data	Most accurate data only
18.5	2	0.5	0.5	0.5	1	1
12.3, 24.6**	3	0.75	0.75	0.5	1.5	1.25
9.25, 18.5, 27.75**	4	1	1	0.5	2	1.5

* For simplicity, no allowance was made here for navigation and elevation displacement.

** Most accurate data (pair).

TABLE 2. AVERAGE ACCURACY.

n	h	All data	Most accurate data only
2	12 km	170	170
3	12 km	94	115
4	12 km	60	98
2	6 km	310	310
3	6 km	168	208
4	6 km	106	174
2	12 km	53	53
3	12 km	29	36
4	12 km	19	30
2	6 km	96	96
3	6 km	52	64
4	6 km	33	54

RIGHT-ANGLE MODE ELEVATION ERROR

In assessing the errors of the right-angle mode of Figure 1, the geometry of Figure 7 defines the measurement problem. As shown in the figure, two flightpaths of equal elevations are assumed to cross at the coordinate system center, P_o . When the aircraft is at point P_1 , an orthogonality error, ψ_1 , exists and similarly when the aircraft is at P_2 an orthogonality error of ψ_2 exists. Since the terrain point at P_T exists in both images, it must lie on circles centered at P_1' and P_2' . It lies, therefore, on the circle defined approximately by the cylinder $R_1^2 = x^2 + z^2$ for small ψ_1 and ψ_2 , and the plane $y = y_1 + m\psi_1$ and also on the circle and plane:

$$R_2^2 = y^2 + z^2, \quad x = x_2 + r\psi_2. \quad (4)$$

Combining these

$$R_1^2 = z^2 + (x_2 + y_1\psi_2)^2, \quad R_2^2 = z^2 + (y_1 + x_2\psi_1)^2, \quad (5)$$

terized as optimistic and realistic, and choosing an average terrain elevation of about 2 km. Again, no advantage was taken of possible block adjustments, although to a first approximation this probably could be assumed to be included in the cost basis.

Fig

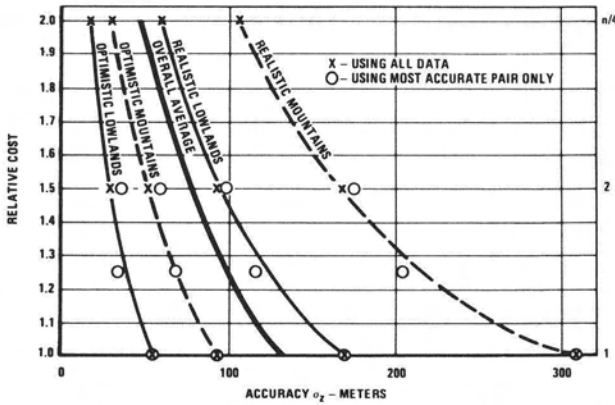


FIG. 6. Cost versus accuracy, parallel equal altitude mode only.

where $m\psi_1 \approx x_2\psi_1$ and $r\psi_2 \approx y_1\psi_2$, neglecting second order effects on the errors.

Taking differentials as before with R , ψ , and z as variables:

$$\begin{aligned} 2R_1 dR_1 &= 2z dz + 2y_1(x_2 + y_1\psi_2) d\psi_2 \\ 2R_2 dR_2 &= 2z dz + 2x_2(y_1 + x_2\psi_1) d\psi_1. \end{aligned} \quad (6)$$

Combining Equations 6

$$\begin{aligned} 4z dz &= 2R_1 dR_1 + 2R_2 dR_2 \\ -2y_1(x_2 + y_1\psi_2) d\psi_2 &- 2x_2(y_1 + x_2\psi_1) d\psi_1. \end{aligned} \quad (7)$$

Figure 7 shows that along-track navigation errors do not cause an elevation error. Across-track and vertical errors do. These may be projected in the direction of R_1 and R_2 . Thus

$$\begin{aligned} dR_{1 \text{ nav}} &= da_1 \frac{h}{R_1} + db_1 \frac{x_2}{R_1} \\ dR_{2 \text{ nav}} &= da_2 \frac{h}{R_2} + db_2 \frac{y_1}{R_2}. \end{aligned} \quad (8)$$

These contributions to the elevation error of Equation 7 are thus

$$\begin{aligned} dR_{1 \text{ nav}} &= 2R_1 \left(\frac{h}{R_1} da_1 + \frac{x_2}{R_1} db_1 \right) \\ dR_{2 \text{ nav}} &= 2R_2 \left(\frac{h}{R_2} da_2 + \frac{y_1}{R_2} db_2 \right) \quad (9) \\ dR_{1 \text{ nav}} &= 2hda_1 + 2x_2db_1, \\ dR_{2 \text{ nav}} &= 2hda_2 + 2y_1db_2. \end{aligned} \quad (10)$$

Now, assuming all differentials represent statistically independent errors and making the following assumptions and approximations,

$$\begin{aligned} y_1\psi_2 &\ll x_2 \\ x_2\psi_1 &\ll y_1 \\ \sigma_{R_1} &\approx \sigma_{R_2} \\ \sigma_{a_1} &\approx \sigma_{a_2} \\ \sigma_{b_1} &\approx \sigma_{b_2} \\ \sigma_{\psi_1} &\approx \sigma_{\psi_2} \end{aligned}$$

$z = h$, altitude above terrain,

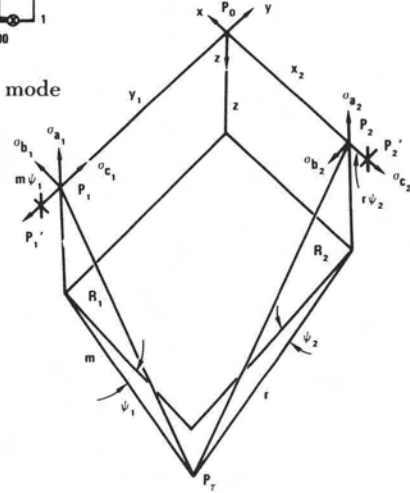


FIG. 7. Right-angle mode geometry.

and combining Equations 7 and 9, dropping the flightpath subscripts

$$\begin{aligned} \sigma_z &= \frac{1}{2h} \left[(x^2 + y^2 + 2h^2) \sigma_R^2 + 2y^2 x^2 \sigma_{\psi^2} \right. \\ &\quad \left. + 2h^2 \sigma_a^2 + (x^2 + y^2) \sigma_b^2 \right]^{1/2}. \end{aligned} \quad (11)$$

Values for this relation in various terrain positions, employing the errors and flight parameters previously used, are given in Figure 8. These values are conservative, in that only one value was used for σ_{ψ} ; viz., 0.1 degree, considered realistic. For cost versus accuracy considerations, the overall averages given are for $n=2$. Double coverage ($n=4$, twice the cost) average error values are those given as $1/4$ area coverages, which are simple averages of the errors for values of x and y up to and including $sw/2$ without redundant data reduction, again conservative.

Comparison of the individual values in Figure 8 with the curves in Figure 4 and comparison of the averages in Figure 8 with the curves in Figure 7 indicates a significant superiority of the right angle mode with respect to the commonly used parallel mode under the assumptions made here. Actual ex-

HIGH MOUNTAINS (6KM)						LOWLANDS																	
						OPTIMISTIC			REALISTIC														
$\frac{x}{y}$	0	SW/4	SW/2	3SW/4	SW	$\frac{x}{y}$	0	SW/4	SW/2	3SW/4	SW	$\frac{x}{y}$	0	SW/4	SW/2	3SW/4	SW						
0	21.3	38.8	57.3	75.9	94.7	0	45.9	78.3	98.5	128.0	158.0	0	38.8	48.7	53.3	67.2	81.6						
SW/4	38.8	72.5	107.4	142.7	178.1	SW/4	78.3	102.3	148.5	181.8	222.5	SW/4	48.7	55.1	73.2	92.8	113.1						
SW/2	57.3	107.4	157.4	211.8	264.4	SW/2	98.5	148.5	191.2	245.4	301.2	SW/2	53.3	73.2	97.8	124.4	152.0						
3SW/4	75.9	142.7	211.8	281.5	351.5	3SW/4	128.0	181.8	245.4	314.4	385.4	3SW/4	67.2	92.8	126.4	158.5	193.8						
SW	94.7	178.1	264.4	351.5	438.0	SW	158.0	222.5	301.2	385.4	472.3	SW	81.6	113.1	152.0	193.8	237.0						
OVERALL AVERAGE = 180.8 1/4 AREA AVERAGE = 73.1						OVERALL AVERAGE = 189.5 1/4 AREA AVERAGE = 186.6						OVERALL AVERAGE = 80.8 1/4 AREA AVERAGE = 37.4						OVERALL AVERAGE = 102.5 1/4 AREA AVERAGE = 57.5					

* AND y VALUES ARE GIVEN HERE IN TERMS OF FRACTIONAL DISTANCE ACROSS THE 37 KM SWATH

FIG. 8. Elevation error summary, right-angle flightpath case.

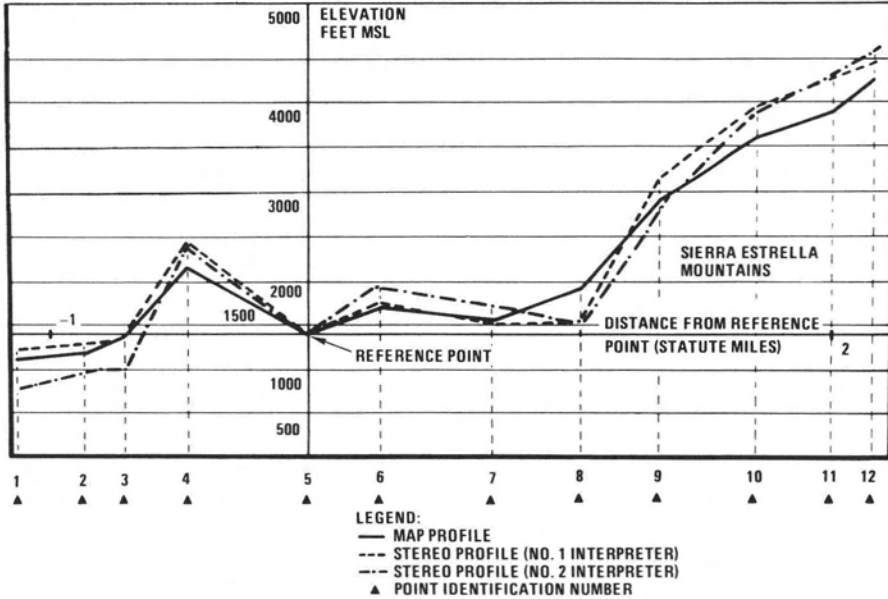


FIG. 9. Terrain profile from GEMS imagery.

perience in collecting and reducing data with both modes under comparable conditions will be required to determine whether the orthogonality assumption is valid and whether adequate fusion for efficient data reduction can be achieved.

EXPERIMENTAL RESULTS

Experimental results of data reduction studies on radar imagery, using block adjustments was reported separately in the 1975 ASP national symposium. Some rather preliminary previous results are reported here for completeness.

Figure 9 shows a 4-mile profile taken from a map sheet, defined by 12 points along the profile. Also shown are two profiles obtained from a radar stereo pair by two radar interpreters by using a simple mirror stereoscope and parallax bar. Since only approximate values of external parameters were available, no absolute measurements could be made. However, by matching the profiles at an ar-

bitrary point, some idea of the potential of the method used with ground control could be made. The result of comparing the map profile with the average of the two interpreters shows an average error of about 40 m over the line which corresponds to that portion of Figure 4 from about 12 km to 20 km. In this range increment, the optimistic curve averages about 50 m.

CONCLUSION

Theory and experiment indicate that currently available terrain-imaging radars have the potential of producing stereo data adequate to permit compilation of at least medium-scale topographic maps. Some versatility exists in choosing imaging modes and flight line spacings. A carefully controlled test over a well-documented test area should be made to further quantify the economic and technical variables and to identify optimum data collection modes and reduction techniques.